



Multigrid Methods for Isogeometric Analysis with THB-Splines

Clemens Hofreither

Institute of Computational Mathematics, Johannes Kepler University
Altenberger Str. 69, 4040 Linz, Austria

Bert Jüttler

Institute of Applied Geometry, Johannes Kepler University
Altenberger Str. 69, 4040 Linz, Austria

Gabor Kiss

Doctoral Program "Computational Mathematics" (W1214)
Johannes Kepler University
Altenberger Str. 69, 4040 Linz, Austria

Walter Zulehner

Institute of Computational Mathematics, Johannes Kepler University
Altenberger Str. 69, 4040 Linz, Austria

Technical Reports before 1998:

1995

- 95-1 Hedwig Brandstetter
Was ist neu in Fortran 90? March 1995
- 95-2 G. Haase, B. Heise, M. Kuhn, U. Langer
Adaptive Domain Decomposition Methods for Finite and Boundary Element Equations. August 1995
- 95-3 Joachim Schöberl
An Automatic Mesh Generator Using Geometric Rules for Two and Three Space Dimensions. August 1995

1996

- 96-1 Ferdinand Kickingger
Automatic Mesh Generation for 3D Objects. February 1996
- 96-2 Mario Goppold, Gundolf Haase, Bodo Heise und Michael Kuhn
Preprocessing in BE/FE Domain Decomposition Methods. February 1996
- 96-3 Bodo Heise
A Mixed Variational Formulation for 3D Magnetostatics and its Finite Element Discretisation. February 1996
- 96-4 Bodo Heise und Michael Jung
Robust Parallel Newton-Multilevel Methods. February 1996
- 96-5 Ferdinand Kickingger
Algebraic Multigrid for Discrete Elliptic Second Order Problems. February 1996
- 96-6 Bodo Heise
A Mixed Variational Formulation for 3D Magnetostatics and its Finite Element Discretisation. May 1996
- 96-7 Michael Kuhn
Benchmarking for Boundary Element Methods. June 1996

1997

- 97-1 Bodo Heise, Michael Kuhn and Ulrich Langer
A Mixed Variational Formulation for 3D Magnetostatics in the Space $H(\text{rot}) \cap H(\text{div})$ February 1997
- 97-2 Joachim Schöberl
Robust Multigrid Preconditioning for Parameter Dependent Problems I: The Stokes-type Case. June 1997
- 97-3 Ferdinand Kickingger, Sergei V. Nepomnyaschikh, Ralf Pfau, Joachim Schöberl
Numerical Estimates of Inequalities in $H^{\frac{1}{2}}$. August 1997
- 97-4 Joachim Schöberl
Programmbeschreibung NAOMI 2D und Algebraic Multigrid. September 1997

From 1998 to 2008 technical reports were published by SFB013. Please see

<http://www.sfb013.uni-linz.ac.at/index.php?id=reports>

From 2004 on reports were also published by RICAM. Please see

<http://www.ricam.oeaw.ac.at/publications/list/>

For a complete list of NuMa reports see

<http://www.numa.uni-linz.ac.at/Publications/List/>

Multigrid Methods for Isogeometric Analysis with THB-Splines

Clemens Hofreither^a, Bert Jüttler^b, Gábor Kiss^c, Walter Zulehner^a

^a*Institute of Computational Mathematics
Johannes Kepler University Linz, Altenberger Str. 69, 4040 Linz, Austria*

^b*Institute of Applied Geometry
Johannes Kepler University Linz, Altenberger Str. 69, 4040 Linz, Austria*

^c*Doctoral Program “Computational Mathematics”
Johannes Kepler University Linz, Altenberger Str. 69, 4040 Linz, Austria*

Abstract

We propose a geometric multigrid algorithm for the solution of the linear systems which arise when using hierarchical spline spaces for isogeometric discretizations of elliptic partial differential equations. In particular, we focus on the use of hierarchical B-spline (HB) and truncated hierarchical B-spline (THB) bases to implement adaptively refined isogeometric discretizations. We describe an approach for constructing the nested sequences of hierarchical spline spaces which are required for our geometric multigrid solver. Furthermore, we give an algorithm for the computation of the so-called prolongation matrices which map coarser-space functions to their finer-space representations for both HB- and THB-spline bases.

In several numerical experiments, we study two-dimensional Poisson problems with singularities and employ a posteriori error estimators for the adaptive refinement of the hierarchical spline spaces. Using standard multigrid smoothers, we observe that using THB-spline bases consistently confers a dramatic advantage in terms of iteration numbers over the use of HB-spline bases, in particular for higher spline degrees.

Keywords: isogeometric analysis, multigrid, hierarchical splines, truncated hierarchical B-splines, adaptive refinement

1. Introduction

Isogeometric analysis (IgA), which was introduced by Hughes [20], is a novel framework for numerical simulation that aims at the close integration of geometry representations from Computer Aided Geometric Design into the analysis process, thereby avoiding the otherwise necessary and expensive data exchange between the FEA and CAD software. However, the tensor product B-spline and NURBS spaces which are most commonly used in geometric design and isogeometric analysis do not provide the possibility of local refinement. Due to their construction, any refinement propagates over the entire domain. To address this issue, other spline spaces which permit local adaptive refinement have been utilized in isogeometric analysis. These include T-splines [1, 9, 28], hierarchical B-splines [2, 26, 27, 30], LR (locally refined) B-splines in [21] and polynomial splines over hierarchical T-meshes [25, 31].

In the present work, we focus on the hierarchical approach to the adaptive refinement of B-splines, which can be traced back to [11]. The key idea of the construction of the hierarchical basis, which was introduced by Kraft [24], consists in a suitable selection of standard tensor-product B-spline functions from a sequence of nested B-spline bases, guided by a sequence of nested subdomains.

The hierarchical B-spline (HB-spline) basis inherits several desirable properties of B-splines such as linear independence, local support and non-negativity. However, it does not possess the partition of unity property and is only weakly stable with respect to the supremum norm.

Email addresses: chofreither@numa.uni-linz.ac.at (Clemens Hofreither), bert.juettler@jku.at (Bert Jüttler), gabor.kiss@dk-compmath.jku.at (Gábor Kiss), zulehner@numa.uni-linz.ac.at (Walter Zulehner)

To overcome these drawbacks, the *truncated hierarchical B-splines* have been recently introduced in [14]. The additional truncation step, which is applied during the construction of the truncated hierarchical basis, ensures that the basis possesses the partition of unity property. In addition, it also improves the stability properties of the basis, see [15], and significantly reduces the overlap between the basis functions from different refinement levels.

For the efficient solution of the large, sparse linear systems arising in isogeometric discretizations, multi-grid methods are an attractive approach. Multigrid solvers for uniformly refined tensor product spline spaces have been studied by several researchers. In particular, geometric multigrid has been considered in [12, 18, 17, 19], and an additive multilevel scheme was proposed in [4]. A symbol-based approach has been taken in [6, 7, 8]. Finally, a local refinement strategy based on full multigrid ideas has been developed in [5].

In the present work, we investigate geometric multigrid solvers for isogeometric discretizations based on adaptively refined hierarchical spline spaces. In particular, we describe how to construct nested sequences of hierarchical spline spaces starting from a coarse tensor product spline space, or from an initial coarse basis used to describe the geometry which may already be hierarchical. We also address the topic of how to compute the necessary prolongation matrices between nested hierarchical spline spaces in both the HB- and the THB-spline bases. As the smoother for the multigrid algorithm, we use a standard Gauss-Seidel method throughout.

We perform several numerical examples and compare the performance of V-cycle multigrid for discretizations based on hierarchical B-spline bases and on truncated hierarchical B-spline bases. Our numerical experiments indicate that using THB-spline bases leads to significantly reduced iteration numbers in the multigrid algorithm compared to using HB-spline bases, especially for higher spline degrees.

The remainder of the paper is structured as follows. In Section 2, we recall some preliminaries on hierarchical spline spaces, truncated hierarchical B-spline bases, and isogeometric analysis. In Section 3, we describe the construction of nested hierarchical spline spaces and a multigrid algorithm over such nested spaces. In Section 4, we give several numerical experiments for adaptively refined discretizations of the Poisson equation. In Section 5, we end with some concluding remarks.

2. Preliminaries

2.1. Bases for hierarchical spline spaces

We consider a sequence

$$S^0 \subset S^1 \subset \dots \subset S^{\Lambda-1} \subset S^\Lambda$$

of nested tensor-product spline spaces of degree $\mathbf{p} = (p_1, \dots, p_d)$ over the parameter domain $D = (0, 1)^d$, where every space S^λ , $\lambda = 0, \dots, \Lambda$ is spanned by normalized B-splines \mathcal{B}^λ and the positive integer Λ specifies the number of levels. (We use Greek characters for the levels in the spline hierarchy in order to keep the Latin ones for the multigrid levels.) Additionally let

$$\Omega = (\Omega^\lambda)_{\lambda \in \mathbb{N}_0}$$

be a sequence of inversely nested subdomains satisfying

$$D = \Omega^0 \supseteq \Omega^1 \supseteq \dots \supseteq \Omega^\Lambda = \emptyset. \quad (1)$$

The first subdomain Ω^0 is the entire parameter domain D . The higher level subdomains represent the regions that are selected for refinement to the level λ .

Each tensor-product spline space S^λ is defined by d knot vectors, one for coordinate direction in the parameter space. These knot vectors are also nested, since this implies the required inclusions of the spline spaces. The knot hyperplanes (knot lines for $d = 2$) determine a segmentation of the domain into cells, and we assume that each subdomain is a collection of cells of the same level. Fig. 1 shows such a hierarchy in the bivariate case for degree $\mathbf{p} = (2, 2)$, as indicated by the three-fold boundary knots, with three levels of refinement.

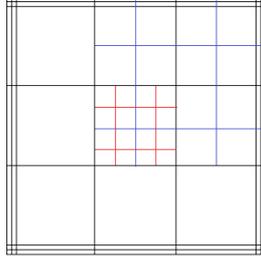


Figure 1: Subdomain structure Ω with 3 hierarchical levels highlighted by black, blue and red for levels 0, 1, 2 respectively.

The hierarchical basis \mathcal{K} , which has been introduced by Kraft [24], with respect to a given subdomain hierarchy Ω is obtained by selecting the *active* B-splines from all levels. A basis function $\beta^\lambda \in \mathcal{B}^\lambda$ is said to be active if

$$\Omega^{\lambda+1} \not\supseteq \text{supp} \beta^\lambda \subseteq \Omega^\lambda,$$

thus

$$\mathcal{K} = \bigcup_{\lambda=0, \dots, \Lambda-1} \{\beta^\lambda \in \mathcal{B}^\lambda : \Omega^{\lambda+1} \not\supseteq \text{supp} \beta^\lambda \subseteq \Omega^\lambda\}.$$

The basis functions collected in \mathcal{K} will be denoted as HB-splines. Fig. 2 shows the construction of the HB-splines for the domain hierarchy shown in Fig. 1.

The HB-splines inherit some of the main properties of the B-splines such as non-negativity, local support and linear independence, as shown in [30]. The partition of unity property and the convex hull property, however, are not preserved during the construction. Nevertheless, they may be recovered, under certain assumptions on the subdomain hierarchy, by a suitable scaling of the basis functions, see [30].

A different approach to restore these properties which does not require any assumptions about the subdomain hierarchy consists in using the *truncated hierarchical B-splines* (THB-splines). In addition, this construction decreases the support overlaps between basis functions from different levels, which will be beneficial for using the multigrid framework, as observed below.

The construction of the THB-splines \mathcal{T} is based on the refinability of B-splines. In fact, any B-spline $\beta \in \mathcal{B}^\lambda$ of level λ can be represented as a linear combination of the B-splines of level $\lambda + 1$ with supports contained in $\text{supp} \beta$, using only non-negative coefficients. Consequently, if a function β of level λ is not active since it satisfies $\text{supp} \beta \subseteq \Omega^{\lambda+1}$, then \mathcal{K} contains functions of higher levels that allow to represent it.

The truncation of a function $\tau \in S^\lambda$ is defined with the help of its representation

$$\tau = \sum_{\beta \in \mathcal{B}^{\lambda+1}} c_\beta^{\lambda+1}(\tau) \beta, \quad c_\beta^{\lambda+1} \in \mathbb{R}.$$

with respect to the basis $\mathcal{B}^{\lambda+1}$. In order to truncate the function, we simply eliminate the contributions of all basis functions that are selected at the higher level

$$\text{trunc}^{\lambda+1} \tau = \sum_{\beta \in \mathcal{B}^{\lambda+1}, \text{supp} \beta \not\subseteq \Omega^{\lambda+1}} c_\beta^{\lambda+1}(\tau) \beta.$$

It may happen that an omitted function $\beta \in \mathcal{B}^{\lambda+1}$ is not active, i.e., not contained in \mathcal{K} . This is the case whenever $\text{supp} \beta \subseteq \Omega^{\lambda+2}$. Nevertheless, this function is still contained in the span of all active functions due to the refinability of B-splines.

We define the THB-splines \mathcal{T} by applying the truncation repeatedly to all functions in \mathcal{K} ,

$$\mathcal{T} = \bigcup_{\lambda=0, \dots, \Lambda-1} \{\text{trunc}^{\Lambda-1}(\text{trunc}^{\Lambda-2} \dots (\text{trunc}^{\lambda+1} \beta^\lambda) \dots) : \beta^\lambda \in \mathcal{K} \cap \mathcal{B}^\lambda\}.$$

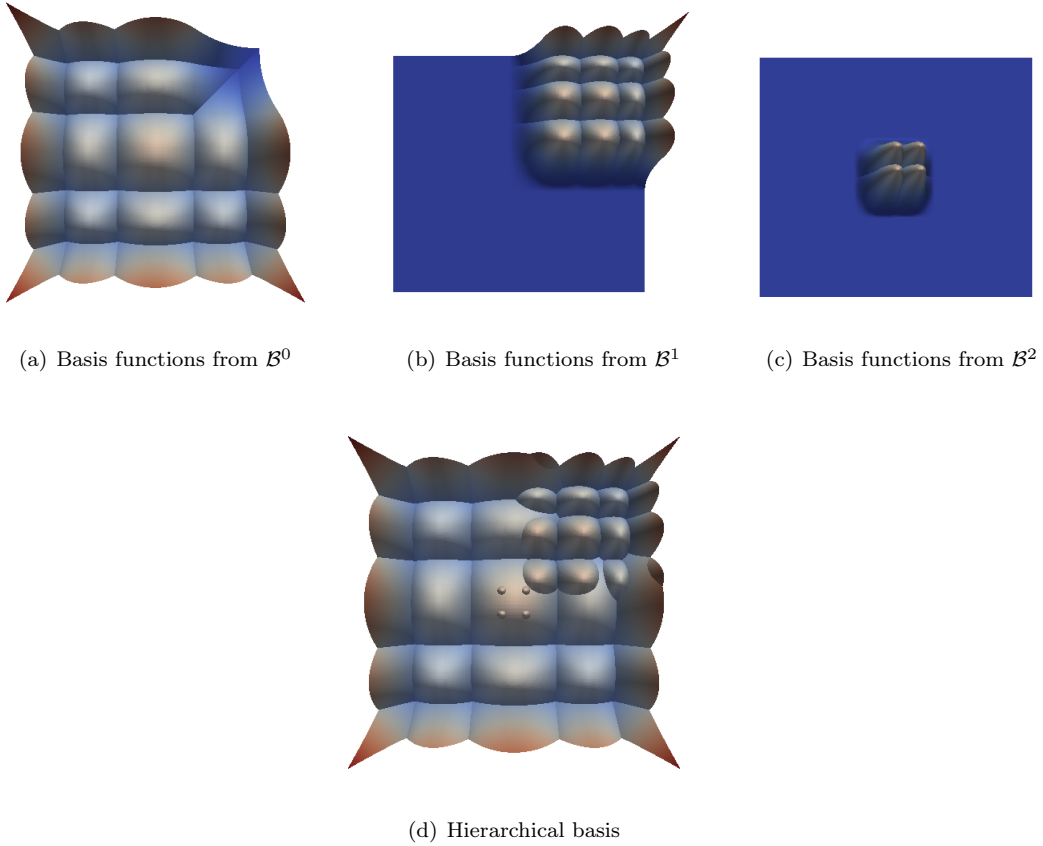


Figure 2: The contribution of basis functions from levels 0, 1 and 2 to the hierarchical basis \mathcal{K} defined over the subdomain structure shown in Figure 1.

In addition to preserving the properties of non-negativity, local support and linear independence, the THB-splines also form a partition of unity [14]. Moreover, the *hierarchical spline spaces* spanned by \mathcal{K} and \mathcal{T} are identical,

$$\text{span } \mathcal{K} = \text{span } \mathcal{T}. \quad (2)$$

Fig. 3 shows the THB-splines for the domain hierarchy in Fig. 1, which is another basis for the space spanned by the HB-splines in Fig. 2.

2.2. Isogeometric analysis

Let

$$G : D \rightarrow G(D) \subset \mathbb{R}^d$$

denote a bijective geometry mapping which maps the parameter domain D to the computational domain $P = G(D)$ on which we wish to solve a boundary value problem. In IGA, this mapping is typically given in terms of spline basis functions, $G \in (S^0)^d$, but its concrete form is irrelevant to our discussion here.

Let $\mathcal{V}_h \subset H_0^1(G(D))$ denote a finite-dimensional space over the computational domain. In isogeometric analysis, this discretization space is obtained by first fixing a family of basis functions $\{\psi_i : D \rightarrow \mathbb{R}\}$ over the parameter domain D and then mapping them into the computational domain via $\varphi_i(x) := \psi_i(G^{-1}(x))$, i.e.,

$$\mathcal{V}_h = \text{span}\{\mathcal{K} \circ G^{-1}\} = \text{span}\{\mathcal{T} \circ G^{-1}\}. \quad (3)$$

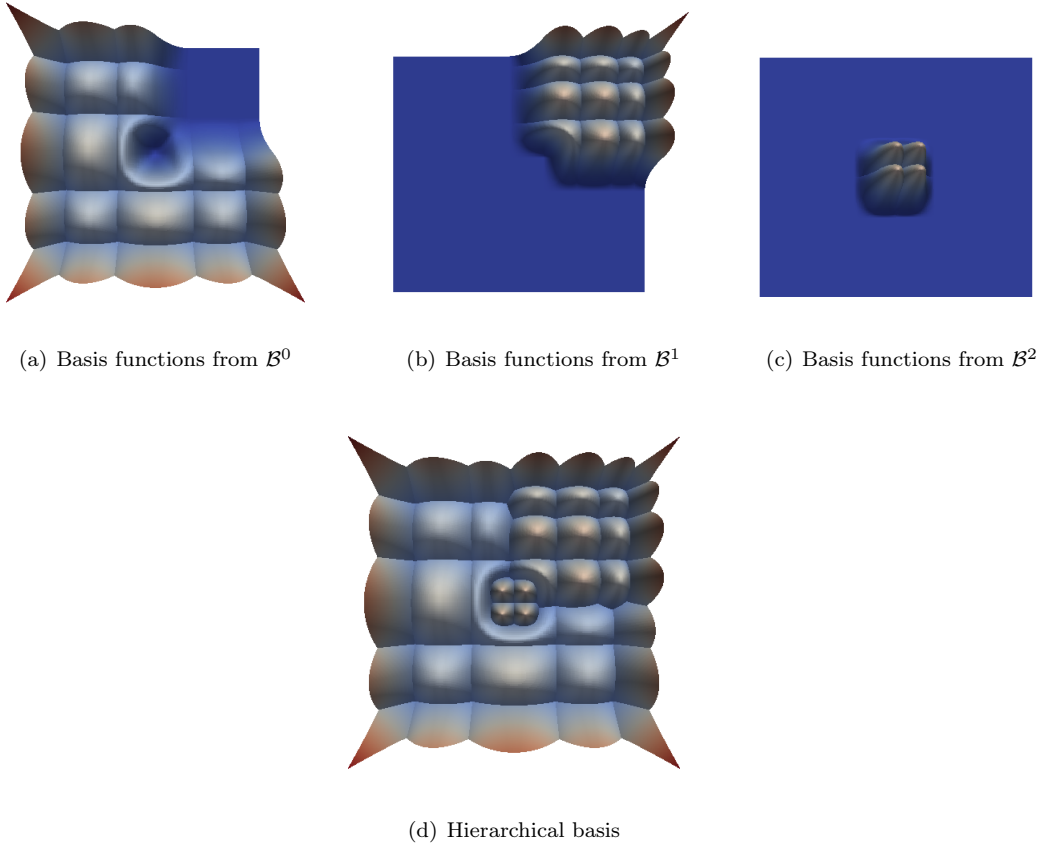


Figure 3: The contribution of basis functions from levels 0, 1 and 2 to the truncated hierarchical B-splines \mathcal{T} defined over the subdomain structure shown in Figure 1. The effect of truncation is clearly visible in the central area of the domain.

Originally, Hughes et al. [20] proposed tensor product B-spline and NURBS bases for $\{\psi_i\}$, and these are still the most popular choices when uniform refinement of the discretization space is desired. In the present work, we instead use hierarchical B-spline and THB-spline bases as described in Subsection 2.1, in order to facilitate local and adaptive refinement of the discretization space.

We now consider an IGA discretization of the Poisson equation with pure Dirichlet boundary conditions: find $u_h \in \mathcal{V}_h$ such that

$$a(u_h, v_h) = \langle F, v_h \rangle \quad \forall v_h \in \mathcal{V}_h \quad (4)$$

with the bilinear form and linear functions, respectively,

$$a(u, v) = \int_P \nabla u \cdot \nabla v \, dx, \quad \langle F, v \rangle = \int_P f v \, dx - a(g, v).$$

Here $g \in H^1(\Omega)$ is a suitable extension of the given Dirichlet data. This discretization results in a large, sparse, symmetric positive definite linear system. Our aim is to investigate geometric multigrid solvers for this system.

3. Multigrid Methods for Adaptively Refined Discretizations

We recall the abstract framework of multigrid methods and describe its realization for hierarchical spline spaces in the isogeometric framework. Special attention is paid to the construction of the prolongation

matrices and the creation of the hierarchy by adaptive refinement.

3.1. An abstract multigrid framework

We recall the construction of a geometric multigrid solver in an abstract setting. We provide only an outline here and refer to the literature [3, 16, 29] for further reading. In later sections, we will flesh out the components of the multigrid solver for our particular setting.

Let $\mathcal{V}_0 \subset H_0^1(G(D))$ denote a coarse discretization space over our computational domain. By a suitable refinement process, we obtain a sequence of nested spaces

$$\mathcal{V}_0 \subset \mathcal{V}_1 \subset \mathcal{V}_2 \subset \dots \subset \mathcal{V}_L. \quad (5)$$

On each level $\ell \in \{0, \dots, L\}$, we denote the number of degrees of freedom by $n_\ell = \dim \mathcal{V}_\ell$. Given a variational formulation of a boundary value problem, we derive a Galerkin discretization in \mathcal{V}_ℓ , resulting in a linear system

$$A_\ell u_\ell = f_\ell,$$

where $A_\ell \in \mathbb{R}^{n_\ell \times n_\ell}$ is the stiffness matrix, $f_\ell \in \mathbb{R}^{n_\ell}$ is the load vector, and $u_\ell \in \mathbb{R}^{n_\ell}$ is the coefficient vector of the discrete solution with respect to a chosen basis for \mathcal{V}_ℓ .

Our aim is to solve the fine-space equation ($\ell = L$) in an efficient manner. The core idea of multigrid is to use an iterative procedure which efficiently reduces (or “smooths”) the high-frequency components of the error, while the low-frequency components of the error are treated by projecting the residual equation to a coarser space. Some of the low-frequency components in the fine space turn into high-frequency components when viewed in the coarser space and can again be efficiently smoothed there. This idea is applied recursively all the way to the coarsest level \mathcal{V}_0 , where the linear system is small enough to solve by a direct method.

Since the spaces are nested, an arbitrary function in \mathcal{V}_ℓ can always be represented on any finer level \mathcal{V}_k , $k > \ell$. Let $P_\ell \in \mathbb{R}^{n_\ell \times n_{\ell-1}}$ denote the *prolongation matrix* which maps the coefficients of a function represented in the basis of $\mathcal{V}_{\ell-1}$ to the coefficients of the same function represented in the basis of \mathcal{V}_ℓ . In other words, P_ℓ realizes the canonical embedding

$$\mathcal{V}_{\ell-1} \rightarrow \mathcal{V}_\ell : v \mapsto v$$

with respect to the particular choice of bases. The transpose of the prolongation matrix P_ℓ^\top is called the *restriction matrix* and maps from the fine to the coarse space. It is easy to show that, when using Galerkin discretizations, the coarse-space stiffness matrix can be obtained via $A_{\ell-1} = P_\ell^\top A_\ell P_\ell$.

As an important ingredient in the multigrid algorithm, we need so-called *smoothers*. On each level except the coarsest, $\ell \in \{1, \dots, L\}$, we choose a smoother $S_\ell \in \mathbb{R}^{n_\ell \times n_\ell}$. This matrix must be easier to invert than the stiffness matrix A_ℓ . Standard choices are the Jacobi smoother, where S_ℓ is chosen as a scalar multiple of the diagonal of A_ℓ , and the Gauss-Seidel smoother, where S_ℓ is chosen as the lower triangular part of A_ℓ . We then define the smoothing operator

$$\mathcal{S}_\ell(v, b) := v + S_\ell^{-1}(b - A_\ell v)$$

for arbitrary vectors and right-hand sides $v, b \in \mathbb{R}^{n_\ell}$. Analogously, we define the transposed smoothing operator $\mathcal{S}_\ell^\top(v, b)$ where the matrix S_ℓ is replaced by its transpose S_ℓ^\top in the definition.

The iterative procedure $v_j \mapsto v_{j+1} := \mathcal{S}_\ell(v_j, b)$ must converge to the solution of the linear system $A_\ell v = b$. Typically, it does so very slowly. However, to obtain an efficient multigrid algorithm it is only required that the smoothing iteration efficiently reduces the components of the error which can not be represented in the coarser space $\mathcal{V}_{\ell-1}$, i.e., the high-frequency error.

We now have the components in place to define the multigrid algorithm in a recursive fashion. On the coarsest level, we define the multigrid operator as the exact solution of the coarse-space problem, i.e.,

$$\mathcal{MG}_0(v, b) := A_0^{-1}b.$$

On every level $\ell > 0$, we define the V-cycle multigrid operator $\mathcal{MG}_\ell(v, b)$ by the sequence of operations

$$\begin{aligned} v^{(1)} &:= \mathcal{S}_\ell(v, b), \\ v^{(2)} &:= v^{(1)} + P_\ell \mathcal{MG}_{\ell-1}(0, P_\ell^\top (b - A_\ell v^{(1)})), \\ \mathcal{MG}_\ell(v, b) &:= v^{(3)} := \mathcal{S}_\ell^\top(v^{(2)}, b). \end{aligned}$$

These three steps are called pre-smoothing, coarse-grid correction, and post-smoothing, respectively. The V-cycle iteration for the fine-grid problem is given, for an arbitrary initial guess $u_0 \in \mathbb{R}^{n_L}$, by the procedure

$$u_{j+1} := \mathcal{MG}_L(u_j, f_L) \quad \forall j = 0, 1, 2, \dots$$

It is called the V-cycle because in each iteration, the method starts with some fine-level approximation $v_j \in \mathbb{R}^{n_L}$, proceeds by smoothing and restriction through all levels to the coarsest space, and then by prolongation and smoothing back to the finest space, obtaining a new approximation $v_{j+1} \in \mathbb{R}^{n_L}$. This pattern can be visualized as a V-shape as in Figure 4.

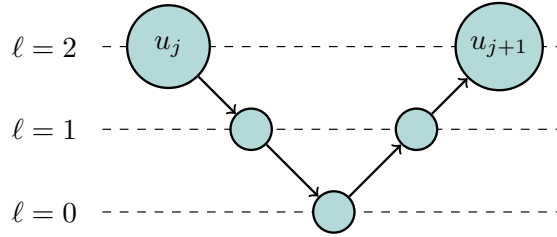


Figure 4: Visualization of one iteration of the multigrid V-cycle algorithm with three nested spaces. Circles correspond to smoothing operations or, on the coarsest level $\ell = 0$, the exact solve. Downward arrows correspond to restriction and upward arrows to prolongation operations.

3.2. Nested sequences of hierarchical spline spaces

The sequence of nested spaces (5) will be generated by performing an isogeometric discretization (with a given geometry mapping) based on nested hierarchical spline spaces (2), which are spanned by (T)HB-splines. More precisely, we use *several* instances of the hierarchical spline spaces (2) which are constructed in a way which ensures that they are nested. The following lemma, which has been derived in [30], will be essential for this construction.

Lemma 1 ([30]). *We consider the two sequences Ω and $\hat{\Omega}$ of nested subdomains*

$$\Omega^0 \supseteq \Omega^1 \supseteq \dots \supseteq \Omega^\Lambda \quad \text{and} \quad \hat{\Omega}^0 \supseteq \hat{\Omega}^1 \supseteq \dots \supseteq \hat{\Omega}^\Lambda$$

and the hierarchical B-splines \mathcal{K} and $\hat{\mathcal{K}}$ defined by them. If $\Omega^\lambda \subseteq \hat{\Omega}^\lambda$ for every $\lambda = 0, \dots, \Lambda$, then

$$\text{span } \mathcal{K} \subseteq \text{span } \hat{\mathcal{K}}.$$

Consequently, enlarging all subdomains of a given subdomain hierarchy Ω while preserving the property that they are nested leads to a superspace of the hierarchical spline space. Clearly, this result is also valid for the THB-splines, as the spaces spanned by HB- and THB-splines are identical (2). Moreover it is also inherited by the spaces used for the isogeometric discretizations (3), since these spaces are obtained simply by composing the hierarchical spline spaces with the inverse of the geometry mappings.

In order to use this result in the multigrid framework, we consider $L + 1$ sequences Ω_ℓ

$$\Omega_\ell = (\Omega_\ell^\lambda)_{\lambda \in \mathbb{N}_0} \quad \text{for } \ell = 0, \dots, L,$$

where each of them satisfies the assumptions specified in Section 2.1. We denote the hierarchical and truncated hierarchical B-splines associated with the sequences Ω_ℓ by \mathcal{K}_ℓ and \mathcal{T}_ℓ , respectively. Furthermore, we make the assumption

$$\Omega_{\ell-1}^\lambda \subseteq \Omega_\ell^\lambda \quad \forall \lambda \in \mathbb{N}_0 \quad \forall \ell \in \mathbb{N}. \quad (6)$$

We combine this with the fact that the subdomains within each hierarchy are also nested, see (1), and obtain the following diagram:

$$\begin{array}{cccccccc}
D = & \Omega_0^0 & \supseteq \dots \supseteq & \Omega_0^\lambda & \supseteq & \Omega_0^{\lambda+1} & \supseteq \dots \supseteq & \Omega_0^\Lambda & = \emptyset \\
& \parallel & & \cap & & \cap & & \parallel & \\
& \vdots & & \vdots & & \vdots & & \vdots & \\
& \parallel & & \cap & & \cap & & \parallel & \\
D = & \Omega_{\ell-1}^0 & \supseteq \dots \supseteq & \Omega_{\ell-1}^\lambda & \supseteq & \Omega_{\ell-1}^{\lambda+1} & \supseteq \dots \supseteq & \Omega_{\ell-1}^\Lambda & = \emptyset \\
& \parallel & & \cap & & \cap & & \parallel & \\
D = & \Omega_\ell^0 & \supseteq \dots \supseteq & \Omega_\ell^\lambda & \supseteq & \Omega_\ell^{\lambda+1} & \supseteq \dots \supseteq & \Omega_\ell^\Lambda & = \emptyset \\
& \parallel & & \cap & & \cap & & \parallel & \\
& \vdots & & \vdots & & \vdots & & \vdots & \\
& \parallel & & \cap & & \cap & & \parallel & \\
D = & \Omega_L^0 & \supseteq \dots \supseteq & \Omega_L^\lambda & \supseteq & \Omega_L^{\lambda+1} & \supseteq \dots \supseteq & \Omega_L^\Lambda & = \emptyset
\end{array}$$

Due to Lemma 1, this yields

$$\text{span}\{\mathcal{K}_0\} \subseteq \dots \subseteq \text{span}\{\mathcal{K}_{\ell-1}\} \subseteq \text{span}\{\mathcal{K}_\ell\} \subseteq \dots \subseteq \text{span}\{\mathcal{K}_L\}$$

and similarly for \mathcal{T}_ℓ . Several comments on this construction of nested hierarchical spline spaces are in order:

- In the standard situation, the sequences Ω_ℓ were constructed by adaptively refining a given uniform discretization consisting of only one level, see Section 3.4. Typically this means that one refinement level is added in every step. Thus we have $\Omega_\ell^\lambda = \emptyset$ whenever $\lambda \geq \ell$. Note that each refinement does not only add an extra level, but may also enlarge the previously introduced subdomains, hence the sets in (6) are generally not equal for $\lambda < \ell$.
- The construction of the multigrid hierarchy also supports geometry mappings which use hierarchical spline spaces, such as the mappings constructed in [10]. In this case, even the coarsest domain hierarchy may be fully populated, i.e., all subdomains are possibly non-empty, except for Ω_0^Λ .
- An alternative multigrid hierarchy can be constructed by considering only the subdomain sequence for the largest level L , i.e., the last row in the diagram. HB-splines \mathcal{K}_L^μ (and similarly THB-splines \mathcal{T}_L^μ) spanning nested discretization spaces are obtained simply by replacing each subdomain Ω_L^λ with the empty set for $\lambda > \mu$. Except for the discretization at the coarsest level, which is the same by definition, this approach gives larger dimensions of the discretization spaces in the multigrid hierarchy. Moreover, it does not comply with the isoparametric principle at all levels if the geometry mapping uses hierarchical splines.

3.3. Computation of the prolongation matrix

In order to describe the computation of the prolongation matrix, which is required for the multigrid solver, we assume that the B-splines within each basis \mathcal{B}^λ are identified by indices, $\mathcal{B}^\lambda = \{\beta_i^\lambda : 1 \leq i \leq m^\lambda\}$, where m^λ is the number of tensor-product B-splines of level λ in the spline hierarchy. Given a fixed level ℓ of the multigrid hierarchy, the active B-splines (which are selected for inclusion in \mathcal{K}_ℓ) are identified by indicator functions

$$\chi_\ell^\lambda(i) = \begin{cases} 1 & \text{if } \beta_i^\lambda \text{ is active in } \mathcal{K}_\ell, \\ 0 & \text{otherwise,} \end{cases} \quad \lambda = 0, \dots, \Lambda.$$

These functions are represented by using a sparse data structure in our implementation, cf. [22]. We also use them to create an index set for the basis functions in \mathcal{K}_ℓ and \mathcal{T}_ℓ ,

$$\mathcal{I}_\ell = \bigcup_{\lambda=0}^{\Lambda} \{\lambda\} \times \mathcal{I}_\ell^\lambda, \quad \mathcal{I}_\ell^\lambda = \{i : \chi_\ell^\lambda(i) = 1, 1 \leq i \leq m^\lambda\}, \quad (7)$$

where \mathcal{I}_ℓ^λ is the index set of active B-spline functions from the hierarchical level λ . The overall index set \mathcal{I}_ℓ of the multigrid hierarchy ℓ is sorted lexicographically with respect to λ and i .

Given two spline hierarchies for adjacent levels $\ell - 1$ and ℓ in the multigrid hierarchy, the algorithm PROLONG computes the associated prolongation matrix for $\mathcal{K}_{\ell-1}$ and $\mathcal{T}_{\ell-1}$:

```

Algorithm PROLONG(  $\mathcal{I}_{\ell-1}, \mathcal{I}_\ell, (R^\lambda)_{\lambda=1, \dots, \Lambda}$  ) {
  //  $\mathcal{I}_{\ell-1}$  and  $\mathcal{I}_\ell$ : index sets of active basis functions of level  $\ell - 1$  and  $\ell$  in the multigrid hierarchy,
  // respectively. The index sets for each level  $\lambda$  in the spline hierarchy are  $\mathcal{I}_{\ell-1}^\lambda$  and  $\mathcal{I}_\ell^\lambda$ , see (7)
  //  $(R^\lambda)_{\lambda=1, \dots, \Lambda}$ : prolongation matrices between  $\mathcal{B}^{\lambda-1}$  and  $\mathcal{B}^\lambda$ , precomputed using knot insertion.
  // The algorithm returns the prolongation matrix  $P_\ell$ .

  create null matrix  $P_\ell$  of size  $|\mathcal{I}_{\ell-1}| \times |\mathcal{I}_\ell|$ 

  for all  $(\lambda, i) \in \mathcal{I}_{\ell-1}$  do {
    create null vector  $M^\lambda$  of size  $m^\lambda$ 
     $M^\lambda[i] := 1$ 
    for  $\nu$  from  $\lambda$  to  $N - 1$  do {
      for all  $k \in \mathcal{I}_\ell^\nu$  do {
        if  $\nu > \lambda$  { // this line THB-splines only
          for all  $k \in \mathcal{I}_{\ell-1}^\nu$  do { // this line THB-splines only
             $M^\nu[k] := 0$  } } // this line THB-splines only
           $P_\ell[(\lambda, i), (\nu, k)] := M^\nu[k]$ 
           $M^\nu[k] := 0$  // this line HB-splines only
        }
      }
       $M^{\nu+1} := R^{\nu+1} M^\nu$  } }

  RETURN( $P_\ell$ ) }

```

For HB-splines, the algorithm iteratively computes the representation of each B-spline in $\mathcal{K}_{\ell-1}$ with respect to the new basis \mathcal{K}_ℓ . This is performed by visiting all levels ν of the spline hierarchy. In each level we eliminate the contributions of the functions which are present at the next level ℓ of the multigrid hierarchy. Subsequently, the remainder is represented with respect to the next level $\nu + 1$ of the spline hierarchy. Clearly, the iteration can be aborted if all coefficients in $M^{\nu+1}$ are zero.

The computation for THB-splines is based on the preservation of coefficients, see [15, Section 5]. We apply truncation to compute the representation at all levels and to determine the coefficients with respect to the THB-splines at level ℓ of the multigrid hierarchy. In order to speed up the computation, we determine, for each index $(\lambda, i) \in \mathcal{I}_{\ell-1}$, the highest level

$$\max\{\lambda' : \text{supp } \beta_i^\lambda \cap \Omega_{\ell'}^{\lambda'} \neq \emptyset\}$$

that can lead to non-zero entries in the prolongation matrix P_ℓ . The iteration is aborted when this level is reached.

3.4. Construction by adaptive refinement

In practice we usually construct the sequence of nested subdomains Ω_ℓ , and therefore the sequence of associated discretization spaces, by adaptive refinement based on an a posteriori error estimator. To this end, we start with a coarse tensor product B-spline discretization defined over the parameter domain. In our notation, this means that the initial hierarchy

$$\Omega_0 = (D)$$

contains only a single domain, namely, the entire parameter domain. Let $\mathcal{V}_0 = \text{span} \mathcal{K}_0$ denote the hierarchical spline space defined over Ω_0 , which is simply a tensor product spline space. Over this coarse space, we solve the discretized boundary value problem (4) and obtain a discrete solution u_0 .

Based on this solution, we compute a residual a posteriori error estimator (see [13] for more details) and refine the parts of the domain where the estimator is largest. This results in a new hierarchy

$$\Omega_1 = (D, \Omega_1^1)$$

which induces a refined hierarchical spline space $\mathcal{V}_1 = \text{span} \mathcal{K}_1 \supseteq \mathcal{V}_0$. We now solve (4) in \mathcal{V}_1 and obtain a new discrete solution u_1 . We repeat the process of a posteriori error estimation and adaptive refinement, adding at most one new level to the hierarchy at each iteration, so that after the k -th step we obtain a hierarchy

$$\Omega_k = (D, \Omega_k^1, \dots, \Omega_k^k)$$

and associated hierarchical spline space $\mathcal{V}_k = \text{span} \mathcal{K}_k$. Note that the refinement procedure may not only add an additional level to the hierarchical spline space, but also enlarge the subdomains associated to the previous levels, as discussed in Section 3.2. We terminate this process once we are satisfied with the accuracy of the obtained solution u_k .

It is clear that the same procedure can be performed when the initial hierarchy Ω_0 is non-trivial, for instance because the geometry map is already given in terms of a hierarchical basis. In our examples, however, we always start from a tensor product space.

3.5. Application of multigrid

The nested sequence of discretization spaces $\mathcal{V}_0 \subset \mathcal{V}_1 \subset \dots \subset \mathcal{V}_k$ constructed in Section 3.4 allows us to apply the abstract multigrid framework described in Section 3.1 to the solution of the discretized problem in \mathcal{V}_k , where $k = L$ is the number of levels in the multigrid hierarchy. For the computation of the transfer matrices P_ℓ which describe the embedding of $\mathcal{V}_{\ell-1}$ in \mathcal{V}_ℓ , we use the procedure described in Section 3.3.

In the present work, we use a simple Gauss-Seidel smoother, i.e., the smoothing matrix S_ℓ used in level ℓ is chosen as the lower triangular part of the stiffness matrix A_ℓ on the same level. It is understood by now that this simple smoothing strategy does not always result in optimal multigrid solvers in the isogeometric setting, in particular for higher spline degrees and space dimensions [19]. However, the design of optimal smoothers for isogeometric analysis is still a field of active research (see, e.g., [17, 7], and we therefore stick to the simple choice of the Gauss-Seidel smoother.

4. Numerical experiments

In this section, we present experimental results for three model problems. Example 1 uses a synthetically generated sequence of meshes generated *a priori*, while Examples 2 and 3 use adaptive refinement by *a posteriori* error estimation for problems with nonsmooth solutions.

In all examples, we compare iteration numbers for THB-spline basis functions with those for HB-spline basis functions. This is a simple change of basis which leaves the discretization spaces unchanged. Throughout we use V-cycle iteration with one pre- and one post-smoothing Gauss-Seidel step on each level. The stopping criterion in all cases is the reduction of the Euclidean norm of the initial residual by a factor of 10^{-8} .

4.1. Example 1

On the square $W = (-1, 1)^2$, we construct a hierarchy of THB-spline spaces by adaptively fitting the function

$$u(x, y) = \exp(52\sqrt{(10x - 2)^2 + (10y - 3)^2})^{-1}$$

starting from a coarse tensor product spline space. The applied fitting method is described in details in [23]. An example of the mesh resulting after several fitting steps is shown in Figure 5.

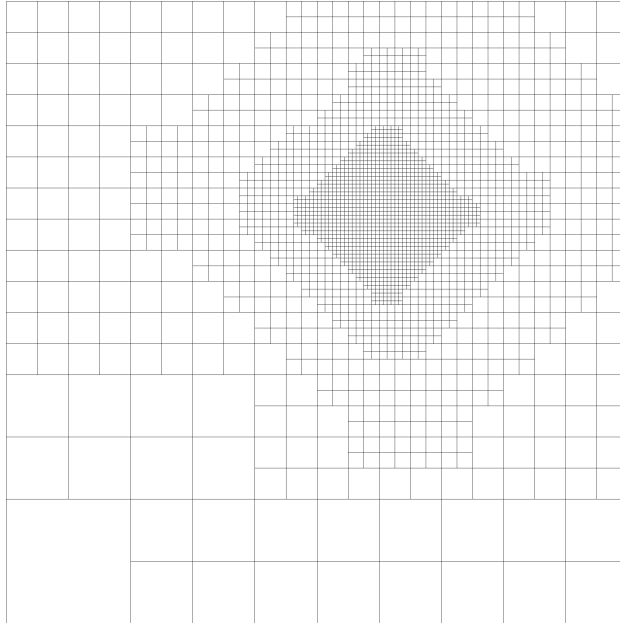


Figure 5: THB-spline supports after five steps of adaptive fitting with quadratic THB-splines (Example 1)

We then solve the Poisson equation

$$-\Delta u = f \quad \text{in } W, \quad u|_{\partial W} = g,$$

where the right-hand side f and Dirichlet data g are chosen according to the exact solution u given above. We use the sequence of nested THB-spline spaces generated by the fitting process as the grids in our multigrid method. Note that in this example, the mesh is refined *a priori* in such a way as to be able to represent the exact solution u well. In the later examples, we will use *a posteriori* error estimators to compute such meshes on the fly.

The iteration numbers are reported in Table 1. When using THB-splines, the number of iterations is significantly smaller than for HB-splines.

4.2. Example 2

We solve the Poisson equation

$$-\Delta u = f \quad \text{in } W, \quad u|_{\partial W} = 0$$

with the source function

$$f(x, y) = \begin{cases} 1, & (x - 0.25)^2 + (y - 1.6)^2 < 0.2^2, \\ 0, & \text{otherwise.} \end{cases}$$

The domain W approximates a quarter annulus in the first quadrant with inner and outer radius 1 and 2, respectively, by means of quadratic tensor product B-splines.

ℓ	$p = 2$			$p = 3$			$p = 4$		
	dofs	THB iter	HB iter	dofs	THB iter	HB iter	dofs	THB iter	HB iter
0	49			64			81		
1	109	11	27	169	43	43	196	167	167
2	365	15	48	475	90	554	528	891	12443
3	829	12	31	1174	75	441	1272	628	13126
4	1487	13	29	2266	81	414	2509	404	10771
5	2317	12	29	3580	75	408	4136	419	9091

Table 1: Iteration numbers for Example 1

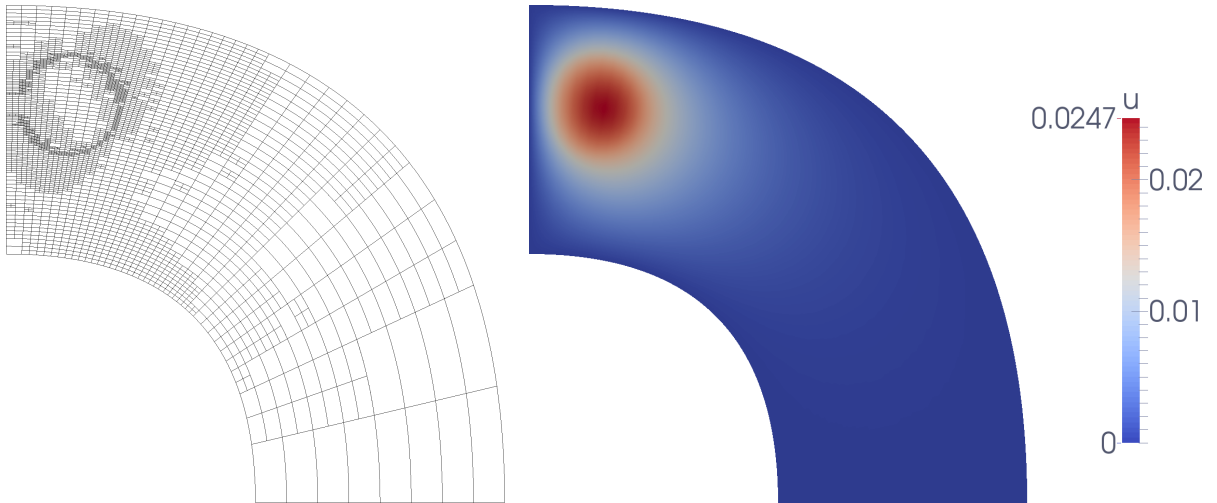


Figure 6: *Left:* Domain from Example 2 with quadratic THB-splines after six adaptive refinement steps (6249 dofs). *Right:* Solution field.

ℓ	$p = 2$			$p = 3$			$p = 4$		
	dofs	THB iter	HB iter	dofs	THB iter	HB iter	dofs	THB iter	HB iter
0	100			121			144		
1	182	15	34	195	68	238	226	183	3656
2	343	18	41	353	75	382	381	397	6112
3	701	24	57	668	131	1176	673	478	6113
4	1355	26	64	1326	198	734	1216	2012	25559
5	2822	23	98	2635	144	987	2312	1436	34310

Table 2: Iteration numbers for Example 2

ℓ	$p = 2$			$p = 3$			$p = 4$		
	dofs	THB iter	HB iter	dofs	THB iter	HB iter	dofs	THB iter	HB iter
0	630			703			780		
1	810	18	33	909	71	297	982	392	3487
2	1163	16	35	1252	68	317	1332	370	3300
3	1631	18	33	1721	84	359	1783	557	4266
4	2338	17	41	2379	73	395	2458	446	5873
5	3327	18	32	3414	87	382	3514	615	6804

Table 3: Iteration numbers for Example 3

Starting from a coarse tensor-product B-spline basis ($\ell = 0$), we construct a hierarchy of THB-spline spaces by means of adaptive refinement based on an *a posteriori* error estimator as described in Section 3.4. An example of a THB-spline basis arising from this adaptive refinement process, as well as a plot of the obtained solution, are shown in Figure 6.

We then set up a multigrid method as described above which always has $\ell = 0$ as its coarse grid and solves the problem on some given level ℓ by V-cycle iteration.

The iteration numbers are reported in Table 2. Once again, when using THB-splines, the number of iterations is significantly smaller than for HB-splines.

4.3. Example 3

We solve the classical benchmark problem for a singularity arising from a reentrant corner on the L-shape domain

$$-\Delta u = 0 \quad \text{in } W, \quad \text{where } W = (-1, 1)^2 \setminus [0, 1]^2.$$

We choose pure Dirichlet boundary conditions according to the exact solution, given in polar coordinates,

$$g(r, \varphi) = r^{2/3} \sin((2\varphi - \pi)/3),$$

where the argument is assumed to have the range $\varphi \in [0, 2\pi)$. The geometry is represented by piecewise linear splines.

We then perform adaptive refinement using THB-splines as described in Example 2. An example of a THB-spline basis arising from adaptive refinement is shown in Figure 7.

The procedure is as in Example 2, and we report the resulting iteration numbers in Table 3, which again confirms the observation regarding the superior performance of THB-splines.

5. Conclusion

We have presented a multigrid solver for isogeometric discretizations of the Poisson equation on adaptively refined hierarchical spline spaces. We have tested the solver both on synthetic examples as well as on hierarchies which were generated by adaptive refinement where the exact solution has a singularity. In each

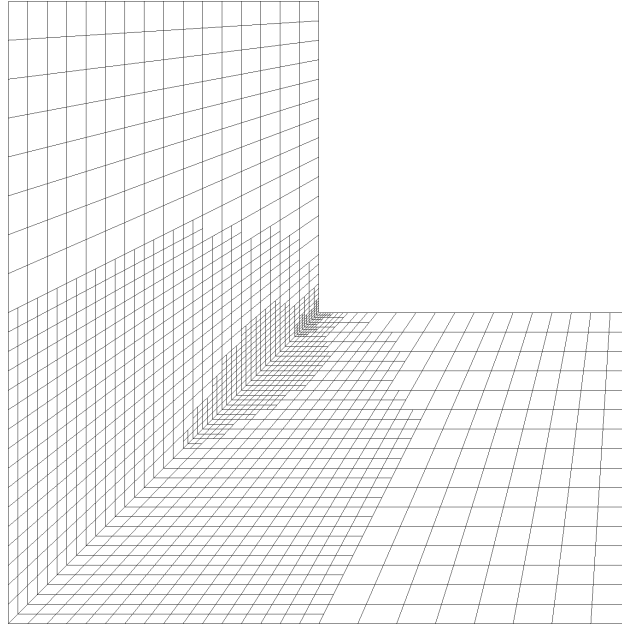


Figure 7: L-shape domain with cubic THB-splines after four adaptive refinement steps (2379 dofs)

example, we compared the iteration numbers when the hierarchical spline space is represented by standard hierarchical B-splines (HB-splines) and by truncated hierarchical B-splines (THB-splines).

In all examples, we found that the V-cycle iteration numbers to reduce the initial residual by a fixed factor were significantly smaller when using THB-splines compared to HB-splines. The difference in iteration numbers was especially dramatic for higher spline degrees. We conjecture that the significantly reduced iteration numbers in the case of THB-splines result from the reduced overlap and consequently lower condition number.

We should point out that for high spline degrees, the iteration numbers are not satisfactory even when using THB-splines. This is consistent with the known fact that even in the case of tensor product B-splines, the Gauss-Seidel smoother does not perform well for high spline degrees [17]. Research into optimal and robust smoothers for isogeometric multigrid methods is ongoing, and we can hope that insights gained in the tensor product case will also result in better smoothers for the more complicated case of hierarchical splines.

Acknowledgments. This work was supported by the National Research Network “Geometry + Simulation” (NFN S117) and by the Doctoral Programme “Computational Mathematics” (W1214), both funded by the Austrian Science Fund (FWF).

References

- [1] Y. Bazilevs, V.M. Calo, J.A. Cottrell, J.A. Evans, T.J.R. Hughes, S. Lipton, M.A. Scott, and T.W. Sederberg. Isogeometric analysis using T-splines. *Computer Methods in Applied Mechanics and Engineering*, 199(5Ü8):229–263, 2010.
- [2] P.B. Bornemann and F. Cirak. A subdivision-based implementation of the hierarchical B-spline finite element method. *Computer Methods in Applied Mechanics and Engineering*, 253:584–598, 2013.
- [3] W. L. Briggs, V. E. Henson, and S. F. McCormick. *A Multigrid Tutorial*. Society for Industrial and Applied Mathematics, 2000.
- [4] A. Buffa, H. Harbrecht, A. Kunoth, and G. Sangalli. BPX-preconditioning for isogeometric analysis. *Computer Methods in Applied Mechanics and Engineering*, 265:63–70, 2013.
- [5] A. Chemin, T. Elguedj, and A. Gravouil. Isogeometric local h-refinement strategy based on multigrids. *Finite Elements in Analysis and Design*, 100:77–90, 2015.

- [6] M. Donatelli, C. Garoni, C. Manni, S. Serra-Capizzano, and H. Speleers. Robust and optimal multi-iterative techniques for IgA Galerkin linear systems. *Computer Methods in Applied Mechanics and Engineering*, 284:230–264, 2014.
- [7] M. Donatelli, C. Garoni, C. Manni, S. Serra-Capizzano, and H. Speleers. Symbol-based multigrid methods for Galerkin B-spline isogeometric analysis. *TW Reports*, 2014.
- [8] M. Donatelli, C. Garoni, C. Manni, S. Serra-Capizzano, and H. Speleers. Robust and optimal multi-iterative techniques for IgA collocation linear systems. *Computer Methods in Applied Mechanics and Engineering*, 284:1120–1146, 2015.
- [9] M.R. Dörfel, B. Jüttler, and B. Simeon. Adaptive isogeometric analysis by local h-refinement with T-splines. *Computer Methods in Applied Mechanics and Engineering*, 199(5-8):264–275, 2010.
- [10] A. Falini, J. Špeh, and B. Jüttler. Planar domain parameterization with THB-splines. *Computer Aided Geometric Design*, 2015. In press. DOI: 10.1016/j.cagd.2015.03.014.
- [11] David R. Forsey and Richard H. Bartels. Hierarchical B-spline refinement. *Computer Graphics (ACM SIGGRAPH)*, 22(4):205–212, 1988.
- [12] K. P. S. Gahalaut, J. K. Kraus, and S. K. Tomar. Multigrid methods for isogeometric discretization. *Computer Methods in Applied Mechanics and Engineering*, 253:413–425, 2013.
- [13] C. Giannelli, B. Jüttler, S.K. Kleiss, A. Mantzaflaris, B. Simeon, and J. Špeh. THB-splines: An effective mathematical technology for adaptive refinement in geometric design and isogeometric analysis. in preparation.
- [14] C. Giannelli, B. Jüttler, and H. Speleers. THB-splines: the truncated basis for hierarchical splines. *Computer Aided Geometric Design*, 29:485–498, 2012.
- [15] C. Giannelli, B. Jüttler, and H. Speleers. Strongly stable bases for adaptively refined multilevel spline spaces. *Advances in Computational Mathematics*, 40(2):459–490, 2014.
- [16] W. Hackbusch. *Multi-Grid Methods and Applications*, volume 4 of *Springer Series in Computational Mathematics*. Springer-Verlag, Berlin, Heidelberg, New York, Tokyo, 2003.
- [17] C. Hofreither and W. Zulehner. Mass smoothers in geometric multigrid for isogeometric analysis. NuMa Report 2014-11, Institute of Computational Mathematics, Johannes Kepler University Linz, Austria, 2014. Accepted for publication in the proceedings of the 8th International Conference Curves and Surfaces.
- [18] C. Hofreither and W. Zulehner. On full multigrid schemes for isogeometric analysis. NuMa Report 2014-03, Institute of Computational Mathematics, Johannes Kepler University Linz, Austria, 2014. Accepted for publication in the proceedings of the 22nd International Conference on Domain Decomposition Methods.
- [19] C. Hofreither and W. Zulehner. Spectral analysis of geometric multigrid methods for isogeometric analysis. In I. Dimov, S. Fidanova, and I. Lirkov, editors, *Numerical Methods and Applications*, volume 8962 of *Lecture Notes in Computer Science*, pages 123–129. Springer International Publishing, 2015.
- [20] T. J. R. Hughes, J. A. Cottrell, and Y. Bazilevs. Isogeometric analysis: CAD, finite elements, NURBS, exact geometry and mesh refinement. *Computer Methods in Applied Mechanics and Engineering*, 194(39-41):4135–4195, October 2005.
- [21] K. A. Johannessen, T. Kvamsdal, and T. Dokken. Isogeometric analysis using LR B-splines. *Computer Methods in Applied Mechanics and Engineering*, 269:471–514, 2014.
- [22] G. Kiss, C. Giannelli, and B. Jüttler. Algorithms and data structures for truncated hierarchical B-splines. In M. Floater et al., editors, *Mathematical Methods for Curves and Surfaces*, volume 8177 of *Lecture Notes in Computer Science*, pages 304–323. Springer, 2014.
- [23] G. Kiss, C. Giannelli, U. Zore, B. Jüttler, D. Großmann, and J. Barner. Adaptive CAD model (re-)construction with THB-splines. *Graph. Models*, 76(5):273–288, 2014.
- [24] R. Kraft. Adaptive and linearly independent multilevel B-splines. In A. Le Mehaute, C. Rabut, and L. L. Schumaker, editors, *Surface Fitting and Multiresolution Methods*, pages 209–218. Vanderbilt University Press, 1997.
- [25] N. Nguyen-Thanh, H. Nguyen-Xuan, S.P.A. Bordas, and T. Rabczuk. Isogeometric analysis using polynomial splines over hierarchical T-meshes for two-dimensional elastic solids. *Computer Methods in Applied Mechanics and Engineering*, 200(21-22):1892–1908, 2011.
- [26] D. Schillinger, L. Dedé, M. A. Scott, J. A. Evans, M. J. Borden, E. Rank, and T. J. R. Hughes. An isogeometric design-through-analysis methodology based on adaptive hierarchical refinement of NURBS, immersed boundary methods, and T-spline CAD surfaces. *Computer Methods in Applied Mechanics and Engineering*, 249:116–150, 2012.
- [27] D. Schillinger, J.A. Evans, A. Reali, M.A. Scott, and T.J.R. Hughes. Isogeometric collocation: Cost comparison with Galerkin methods and extension to adaptive hierarchical NURBS discretizations. *Computer Methods in Applied Mechanics and Engineering*, 267:170–232, 2013.
- [28] M.A. Scott, X. Li, T.W. Sederberg, and T.J.R. Hughes. Local refinement of analysis-suitable T-splines. *Computer Methods in Applied Mechanics and Engineering*, 213-216:206–222, 2012.
- [29] U. Trottenberg, C.W. Oosterlee, and A. Schüller. *Multigrid*. Academic Press, 2001.
- [30] A.-V. Vuong, C. Giannelli, B. Jüttler, and B. Simeon. A hierarchical approach to adaptive local refinement in isogeometric analysis. *Computer Methods in Applied Mechanics and Engineering*, 200:3554–3567, 2011.
- [31] P. Wang, J. Xu, J. Deng, and F. Chen. Adaptive isogeometric analysis using rational PHT-splines. *Computer-Aided Design*, 43(11):1438–1448, 2011.

Latest Reports in this series

2009 - 2013

[..]

2014

[..]

- | | | |
|---------|---|----------------|
| 2014-05 | Irina Georgieva and Clemens Hofreither
<i>Interpolating Solutions of the Poisson Equation in the Disk Based on Radon Projections</i> | July 2014 |
| 2014-06 | Wolfgang Krendl and Walter Zulehner
<i>A Decomposition Result for Biharmonic Problems and the Hellan-Herrmann-Johnson Method</i> | July 2014 |
| 2014-07 | Martin Jakob Gander and Martin Neumüller
<i>Analysis of a Time Multigrid Algorithm for DG-Discretizations in Time</i> | September 2014 |
| 2014-08 | Martin Jakob Gander and Martin Neumüller
<i>Analysis of a New Space-Time Parallel Multigrid Algorithm for Parabolic Problems</i> | November 2014 |
| 2014-09 | Helmut Gfrerer and Jiří V. Outrata
<i>On Computation of Limiting Coderivatives of the Normal-Cone Mapping to Inequality Systems and their Applications</i> | December 2014 |
| 2014-10 | Clemens Hofreither and Walter Zulehner
<i>Spectral Analysis of Geometric Multigrid Methods for Isogeometric Analysis</i> | December 2014 |
| 2014-11 | Clemens Hofreither and Walter Zulehner
<i>Mass Smoothers in Geometric Multigrid for Isogeometric Analysis</i> | December 2014 |

2015

- | | | |
|---------|--|---------------|
| 2015-01 | Peter Gangl, Ulrich Langer, Antoine Laurain, Houcine Meftahi and Kevin Sturm
<i>Shape Optimization of an Electric Motor Subject to Nonlinear Magnetostatics</i> | January 2015 |
| 2015-02 | Stefan Takacs and Thomas Takacs
<i>Approximation Error Estimates and Inverse Inequalities for B-Splines of Maximum Smoothness</i> | February 2015 |
| 2015-03 | Clemens Hofreither, Ulrich Langer and Steffen Weißer
<i>Convection-adapted BEM-based FEM</i> | February 2015 |
| 2015-04 | Helmut Gfrerer and Boris S. Mordukhovich
<i>Complete Characterizations of Tilt Stability in Nonlinear Programming under Weakest Qualification Conditions</i> | March 2015 |
| 2015-05 | Matúš Benko and Helmut Gfrerer
<i>An SQP Method for Mathematical Programs with Complementarity Constraints with Strong Convergence Properties</i> | May 2015 |
| 2015-06 | Irina Georgieva and Clemens Hofreither
<i>An Algorithm for Low-rank Approximation of Bivariate Functions Using Splines</i> | May 2015 |
| 2015-07 | Elias Karabelas and Martin Neumüller
<i>Generating Admissible Space-Time Meshes for Moving Domains in $d + 1$-Dimensions</i> | May 2015 |
| 2015-08 | Clemens Hofreither, Bert Jüttler, Gabor Kiss and Walter Zulehner
<i>Multigrid Methods for Isogeometric Analysis with THB-Splines</i> | June 2015 |

From 1998 to 2008 reports were published by SFB013. Please see

<http://www.sfb013.uni-linz.ac.at/index.php?id=reports>

From 2004 on reports were also published by RICAM. Please see

<http://www.ricam.oeaw.ac.at/publications/list/>

For a complete list of NuMa reports see

<http://www.numa.uni-linz.ac.at/Publications/List/>